Synchronization in Coupled Maps with Triangular Networks

Yoko Uwate[†] and Yoshifumi Nishio[†]

†Dept. of Electrical and Electronic Engineering, Tokushima University
2-1 Minami-Josanjima, Tokushima, Japan
Email: {uwate, nishio}@ee.tokushima-u.ac.jp

Abstract—In this study, we investigate synchronization phenomena when the 2-dimensional maps based on neuron model are coupled with triangular network property. Furthermore, the difference of synchronization obtained from the coupled maps and the coupled oscillators is compared.

1. Introduction

Generally, complex dynamical phenomena can be observed in networks formed by many elements with nonlinearity. Coupled Map Lattice (CML) has proposed by Kaneko and Bunimovich [1]-[5], to use as general models for the complex high-dimensional dynamics, such as biological systems, networks in DNA, economic activities, neural networks, and evolutions. We can observe the spatio-temporal patterns in CML. Moreover, coupled oscillatory systems can also produce interesting phase patterns, including wave propagation, clustering, and complex phase patterns. It is very important to make clear this mechanism of these spatio-temporal patterns for understanding complex patterns observed in natural science. Usually, the chaotic maps are used for CML and many interesting spatio-temporal patterns were observed.

Recently, a discrete map for spiking-bursting neural behavior was proposed by Rulkov [6], [7]. Rulkov map (see. Fig. 1) in the form of a two-dimensional map can be useful for understanding the dynamical mechanism of oscillators in the large scale networks. And Rulkov map produce spiking-bursting behavior such as real neurons.

In this study, we investigate synchronization phenomena when the 2-dimensional maps based on neuron model are coupled with triangular network property. Furthermore, the difference of synchronization obtained from the coupled maps and the coupled oscillators is compared.

2. Coupled Maps with Triangular Networks

The several types of coupled maps with triangular networks are shown in Fig. 2.

We consider a chain of coupled maps:

$$x_{i,n+1} = f(x_{i,n}x_{i,n-1}, y_{i,n})$$
$$+ \frac{1}{2}g(x_{i+1,n} - 2x_{i,n} + x_{i-1,n}),$$
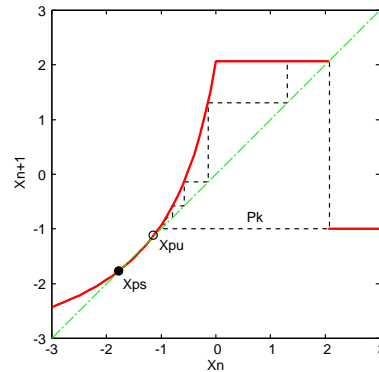$$y_{i,n+1} = y_{i,n} - \mu(x_{i,n} + 1) + \mu\sigma_i$$

Figure 1: Rulkov map. The dashed line illustrates a super-stable cycle P_k. The stable and unstable fixed points of the map are indicated by x_{ps} and x_{pu}, respectively.
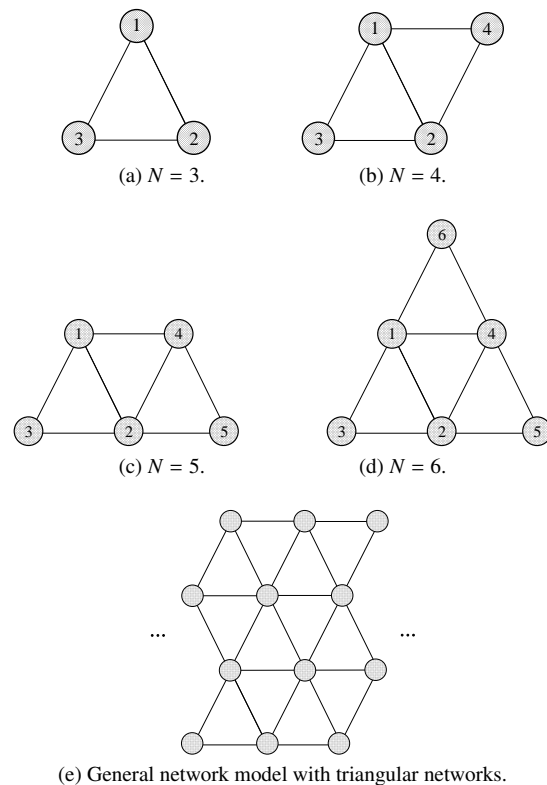

(a) $N = 3$.

(b) $N = 4$.

(c) $N = 5$.

(d) $N = 6$.

(e) General network model with triangular networks.

Figure 2: Several types of coupled maps with triangular network property.

$$+\mu\frac{1}{2}g(x_{i+1,n}-2x_{i,n}+x_{i-1,n}),$$
$$i=1,...,N, \tag{1}$$

where x and y are the fast and slow dynamical variables, respectively. $\mu = 10^{-3}$ and σ_i are the parameters of the individual map and g is the coupling. The function $f()$ has the following form:

$$f(x_n, y_n) = \begin{cases} \alpha/(1-x_n)+y_n, & x_n \le 0, \\ \alpha+y_n, & 0 < x_n < \alpha+y_n \\ & and \ x_{n-1} \le 0, \\ -1, & x_n \ge \alpha+y_n \ or \ x_{n-1} > 0, \end{cases} \tag{2}$$

In this simulations, we take $\alpha = 3.5$ and σ_i is set for randomly distributed in the interval [0.15:0.16].

2.1. Synchronization for $N = 3$

First, we consider the simplest model as shown in Fig. 2(a). The three maps are coupled as ring topology. In this coupled maps model, three phase synchronization can be observed when the copuling strength is set to $g = -0.029$.
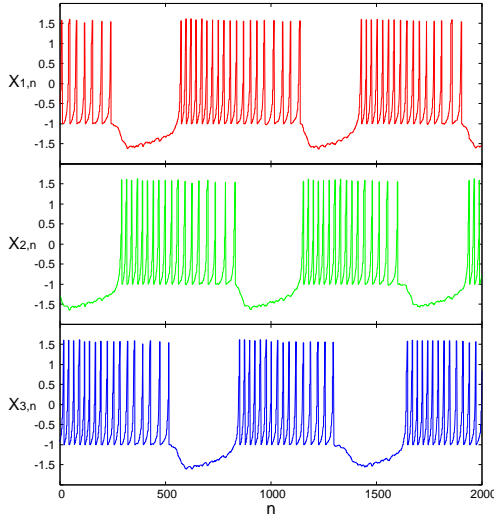

Figure 3: Three-phase synchronization ($g = -0.029$).

2.2. Synchronization for $N = 4$

Next, the model of coupled maps with two triangular networks as shown in Fig. 2 (b) is considered. We observe two types of synchronization states dependence on the value of σ. When σ is fixed with 0.24, two pair of three phase synchronization is obtained. The time wave forms of each map are shown in Fig. 4. From this figure, the first, the second and the third maps are synchronized with three-phase state. Also, the first, the second and the fourth maps synchronize at three-phase. Furthermore, we confirm that the third and the fourth maps are synchronized with in-phase state.

While, in the case of $\sigma = 0.10$, in/anti phase synchronization can be observed as shown in Fig. 5. The first and the second maps are synchronized at the in-phase state and the other combinations are synchronized at the anti-phase state.
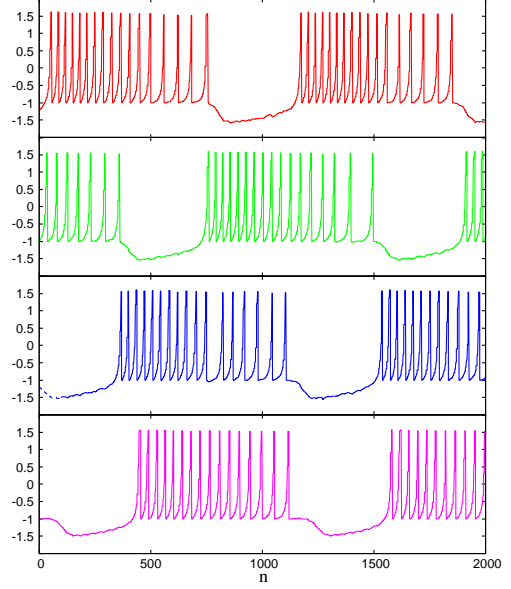

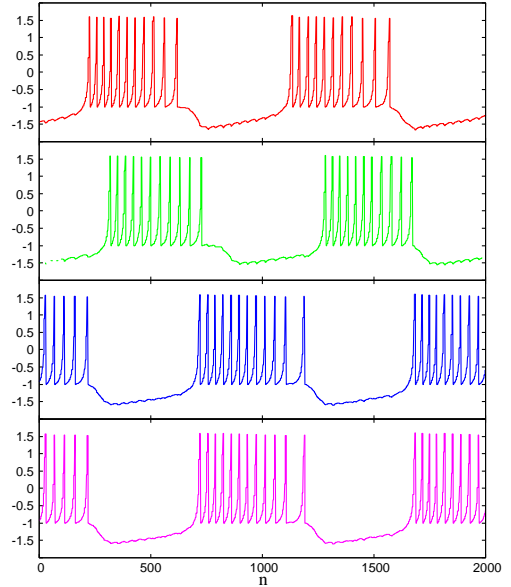Figure 4: Two pair of three-phase synchronization ($\sigma = 0.24$).

Figure 5: In/Anti-phase synchronization ($\sigma = 0.10$).

3. Comparison with Coupled Oscillatory System

In this section, we compare synchronization phenomena between the coupled maps and the coupled oscillators.

3.1. Circuit Model for $N = 3$

The circuit model of three coupled van der Pol oscillator as ring topology is shown in Fig. 6. This circuit model corresponds to the three coupled maps shown in Fig. 2 (a).
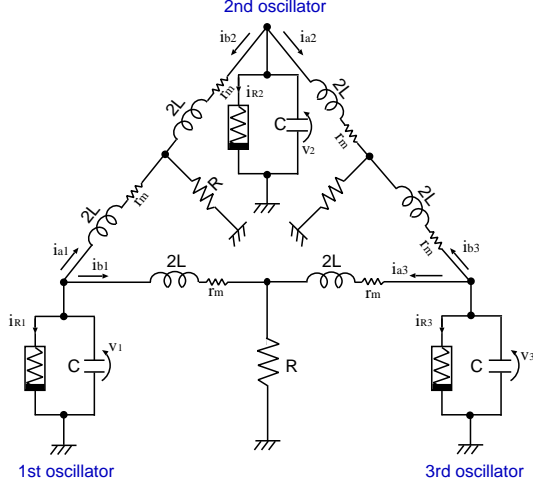

Figure 6: Circuit model ($N = 3$).

We assume that the $v_k - i_{Rk}$ characteristics of the nonlinear resistor in each oscillator is given by the following third order polynomial equation,

$$i_{Rk} = -g_1 v_k + g_3 v_k^3 \quad (g_1, g_3 > 0),\tag{3}$$

$$(k = 1, 2, 3, 4).$$

The normalized circuit equations governing the circuit are expressed as

[First oscillator]

$$\begin{cases} \dfrac{dx_1}{d\tau} = \varepsilon\left(1 - \dfrac{1}{3}x_1{}^2\right)x_1 - (y_{a1} + y_{b1}) \\[2mm] \dfrac{dy_{a1}}{d\tau} = \dfrac{1}{2}\left\{x_1 - \eta y_{a1} - \beta\gamma(y_{a1} + y_{b2})\right\} \\[2mm] \dfrac{dy_{b1}}{d\tau} = \dfrac{1}{2}\left\{x_1 - \eta y_{b1} - \gamma(y_{a3} + y_{b1})\right\} \end{cases}\tag{4}$$

[Second oscillator]

$$\begin{cases} \dfrac{dx_2}{d\tau} = \varepsilon\left(1 - \dfrac{1}{3}x_2{}^2\right)x_2 - (y_{a2} + y_{b2}) \\[2mm] \dfrac{dy_{a2}}{d\tau} = \dfrac{1}{2}\left\{x_2 - \eta y_{a2} - \gamma(y_{a2} + y_{b3})\right\} \\[2mm] \dfrac{dy_{b2}}{d\tau} = \dfrac{1}{2}\left\{x_2 - \eta y_{b2} - \beta\gamma(y_{a1} + y_{b2})\right\} \end{cases}\tag{5}$$

[Third oscillator]

$$\begin{cases} \dfrac{dx_3}{d\tau} = \varepsilon\left(1 - \dfrac{1}{3}x_3{}^2\right)x_3 - (y_{a3} + y_{b3}) \\[2mm] \dfrac{dy_{a3}}{d\tau} = \dfrac{1}{2}\left\{x_3 - \eta y_{a3} - \gamma(y_{a3} + y_{b1})\right\} \\[2mm] \dfrac{dy_{b3}}{d\tau} = \dfrac{1}{2}\left\{x_3 - \eta y_{b3} - \gamma(y_{a2} + y_{b3})\right\} \end{cases}\tag{6}$$

where

$$t = \sqrt{LC}\tau, \quad v_k = \sqrt{\dfrac{g_1}{3g_3}}x_k,$$

$$i_{ak} = \sqrt{\dfrac{g_1}{3g_3}}\sqrt{\dfrac{C}{L}}y_{ak}, \quad i_{bk} = \sqrt{\dfrac{g_1}{3g_3}}\sqrt{\dfrac{C}{L}}y_{bk},$$

$$\varepsilon = g_1\sqrt{\dfrac{L}{C}}, \quad \gamma = R\sqrt{\dfrac{C}{L}}, \quad \eta = r_m\sqrt{\dfrac{C}{L}},$$

$$(k = 1, 2, 3).$$

In this equations, γ is the coupling strength and ε denotes the nonlinearity of the oscillators. For the computer simulations, γ and ε are fixed with 0.1, 0.1, respectively. For the computer simulations, we calculates Eqs. (4)-(6) using a fourth-order Runge-Kutta method with the step size $h = 0.005$. Figure 7 shows the three time wave forms obtained by each oscillator. We can see that the three oscillators are synchronized at the three-phase state.
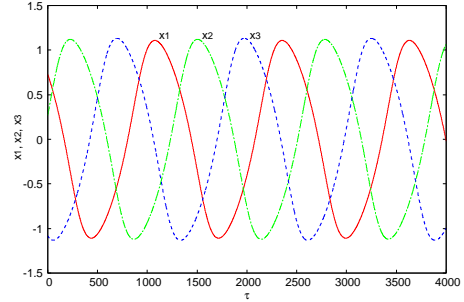

Figure 7: Three phase synchronization obtained from coupled oscillatory system.

3.2. Circuit Model for $N = 4$

Here, we consider the two coupled triangle oscillatory networks sharing a branch. The circuit model of two coupled triangle oscillatory networks sharing the branch is shown in Fig. 8.
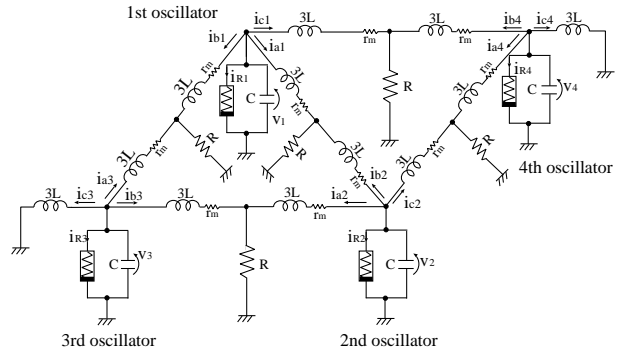

Figure 8: Circuit model ($N = 4$).

The parameters of this circuit model are fixed as $\varepsilon = 0.1$, $\gamma = 0.1$, $\eta = 0.0001$.

Figure 9 shows the time wave form of the voltage charged at the capacitance of each oscillator. From this figure, we can see that the first and the second oscillators are synchronized at in-phase (phase difference: 0 degree). While, the other combination oscillators synchronize with anti-phase (phase difference: 180 degree). Furthermore, the amplitude of between the first/second and the third/fourth oscillators has small difference. The phase plane of each combination oscillator is shown in Fig. 10.
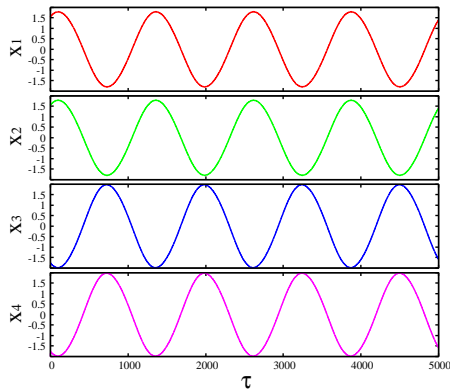

Figure 9: Time wave form of the voltage charged at the capacitance of each oscillator.
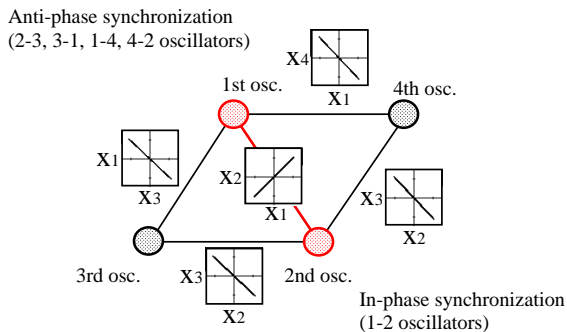

Figure 10: Phase plane of each oscillator.

4. Discussions

In this section, we compare the synchronization phenomena between the coupled maps system and the coupled oscillators system. In the case of that the number of coupled elements is $N = 3$, the three-phase synchronization can be observed from the both systems. When the number of coupled elements is fixed as $N = 4$, we observe the in/anti-phase synchronization from the both systems. Furthremore, the two pair of three-phase synchronization can be observed from the coupled maps system.

5. Conclusions

In this study, we have investigated synchronization phenomena when the 2-dimensional maps based on neuron model are coupled with triangular network property. Furthermore, the difference of synchronization obtained from the coupled maps and the coupled oscillators was compared.

References

[1] K. Kaneko, "Spatiotemporal Intermittency in Coupled Map Lattice," Prog. Theor. Phys., vol.75, no.5, pp.1033–1044, 1985.

[2] L. A. Bunimovich and Ya. G. Sinai, "Spacetime Chaos in Coupled Map Lattices," Nonlineality 1, no.4, pp.491–516, 1988.

[3] K. Kaneko, "Pattern Dynamics in Spatiotemporal Chaos," Physica D, vol.34, pp.1–41, 1989.

[4] K. Kaneko, "Spatiotemporal Chaos in One- and Two- Dimensional Coupled Map Lattice," Physica D, vol.37, pp.60–82, 1989.

[5] K. Kaneko, "Simulating Physics with Coupled Map Lattice - Pattern Dynamics, Information Flow, and Thermodynamics of Spatiotemporal Chaos," Formation, Dynamics, and Statistics of Patterns, World Sci., pp.1–52, 1990.

[6] N. F. Rulkov, "Modeling of Spiking-Bursting Neural Behavior using Two-dimensional Map," Physical Rev., E, vol. 65, 041922, 2002.

[7] N. F. Rulkov, I. Timofeev and M. Bazhenov, "Oscillations in Large-Scale Cortical Networks: Map-Based Model," Journal of Computational Neuroscience vol. 17 pp. 203–223, 2004.